12th International Conference on Advances in Steel-Concrete Composite Structures (ASCCS 2018)
Universitat Politècnica de València, València, Spain, June 27-29, 2018
Doi: http://dx.doi.org/10.4995/ASCCS2018.2018.6986

Pull-out Behaviour of Extended Hollobolts for Hollow Beam-Column Connections

M. F. Shamsudin[a,b]* and W. Tizani[a]

[a]Department of Civil Engineering, The University of Nottingham, UK
[b]Department of Civil Engineering, University of Malaya, Malaysia
*corresponding author, e-mail address: evxmfs@nottingham.ac.uk

Abstract

The use of structural hollow sections (SHS) as columns in single-storey and multi-storey results in better compression strength, low surface area, architectural attractiveness and high strength to weight ratio. One major constraint when connecting to hollow sections is in accessing and tightening the bolt from the inside of the hollow section. To resolve this issue, full welding is usually applied. But this may suffer from high labour cost, and the potential of low quality welding due to workmanship and varied environmental conditions. Connecting using additional components, such as gusset plates and brackets, helps to ease this problem but lowers aesthetic appeal. To avoid the need to access to the inner face of the column section, new type of fasteners known as blind bolts were introduced. In this paper, experimental and numerical studies were conducted using a new anchored blind bolt known as the Extended HolloBolt (EHB), with the objective of using the component method for predicting joint behaviour within the tensile region. The behaviour of EHB in a group with different connection topologies and configurations was investigated using a total of 36 tests with one row of M16 Grade 8.8 and 10.9 bolts subjected to pull-out loading in tension. The experimental work covers a range of parameters such as bolt gauge, concrete strength, concrete type, bolt embedment depth and bolt class. A finite element model was implemented with good agreement between experimental and simulated load-deflection results, which have a maximum difference of 2.5%, shows that the model is suitable to be used for parametric studies or analytical work in further research on the EHB.

Keywords: *Hollow sections; Blind bolts; Extended Hollobolt; Component Method.*

1. Introduction

The use of structural hollow sections (SHS) as columns in single-storey and multi-storey results in better compression strength, low surface area, architectural attractiveness and high strength to weight ratio. One major constraint when connecting to hollow sections is in accessing and tightening the bolt from the inside of the hollow section. To resolve this issue, full welding is usually applied. But this may suffer from high labour cost, the potential of low on-site welding quality due to variability of workmanship and environmental conditions. Connecting using additional components, such as gusset plates and brackets, helps to ease this problem but lower aesthetic appeal. To meet the need to access to the inner column section from one side only, new type of fasteners known as blind bolts were introduced.

Blind bolts have been introduced as alternative fasteners to connect with hollow column face and have been proven to work well in simple connections. The commercially modified Lindapter HolloBolt, termed as the Extended HolloBolt (EHB) offers better tensile performance in term of capacity, stiffness, and ductility while possessesing similar shear capacity to standard bolts [1]. As the EHB is relatively recent, there remain many areas that require further research. With this in mind, this paper presents some experimental pull-out tests and numerical modelling using the finite element (FE) method.

2. Experimental program.

2.1. Extended HolloBolt (EHB) Connection

The behavior of the extended HolloBolt (EHB) depends on three individual elements; i) internal bolt elongation, which depends on material properties of bolt shank, (ii) flaring sleeves which facilitates resistance from pulling-out of internal bolt, and it tends to displace and slip in high shear stresses, iii) bond and anchorage which provides a bond resistance as a result of head bearing stress between the concrete and the anchor nut. Previous studies showed that EHB provide higher bond contribution than other type of bolts [2]. The EHB has proved to have significantly enhanced stiffness compared with the standard HolloBolt [3, 4].

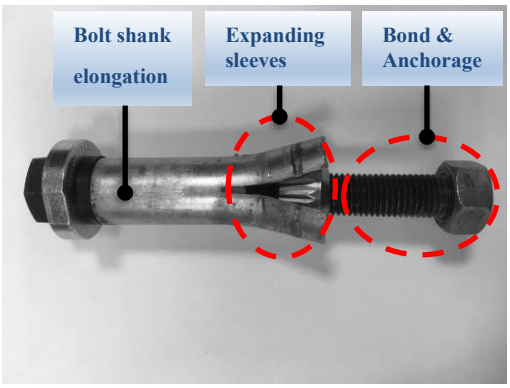

Fig. 1. Component mechanism

2.2. Concrete-filled Hollow Section

The concrete-filled column combines the advantages of the ductile steel frames with the high compressive strength of concrete components, which acts to reduce drift [5]. The interaction between steel tube and concrete has been shown to cause a delay in the local buckling of the steel tube due to the restraint provided by the concrete [6]. This delay helps to increase the stiffness and strength of the composite structure. Apart from that, the use of steel tube column removes the requirement of formworks during construction process [7]. By filling the tube eliminates the flexibility of the tube face and by extending and anchoring the blind bolt in the concrete, the tensile stiffness and resistance of the blind bolt is improved. Hence can allow for moment resisting connections.

2.3. Test specimens

The experimental investigation of the EHB in tension is performed by applying a pull-out load to the EHBs. A standard tensile pull-out test was performed to evaluate the stiffness, strength and ductility of bolts in concrete. All the tests were performed using bolt diameter M16. The setup involves a steel box simulating rectangular hollow sections (RHS). The box comprised of flat plates which are bolted to parallel flange channel sections. There are three justifications for the selection of steel box assembly: (1) to provide confinement to the concrete; (2) to eliminate concrete splitting failure; (3) to allow access to inspect tested specimens by simply unbolting its sections.

To ensure that the behaviour of the blind-bolts alone is investigated, a 40mm thick top plate and 50 mm counter bore thick tee stub are provided in the test setup.

Eighteen samples were tested covering all the study parameters, as shown in *Table 1*. The concrete mix was designed to have the required compressive strength at the time of testing.

Table 1. Test matrix

No.	Bolt gauge Distance (mm)	Concrete grade	d_{emb} (mm)
1	120	C20	66
2	140	C20	66
3	180	C20	66
4	120	C40	66
5	140	C40	66
6	120	C80	66
7	140	C80	66
8	180	C80	66
9	120	C20	76
10	140	C20	76
11	180	C20	76
12	120	C20	86
13	140	C20	86
14	180	C20	86
15	120	Lightweight C30	66
16	140	Lightweight C30	66
17	180	Lightweight C30	66
18	120	Without concrete	66

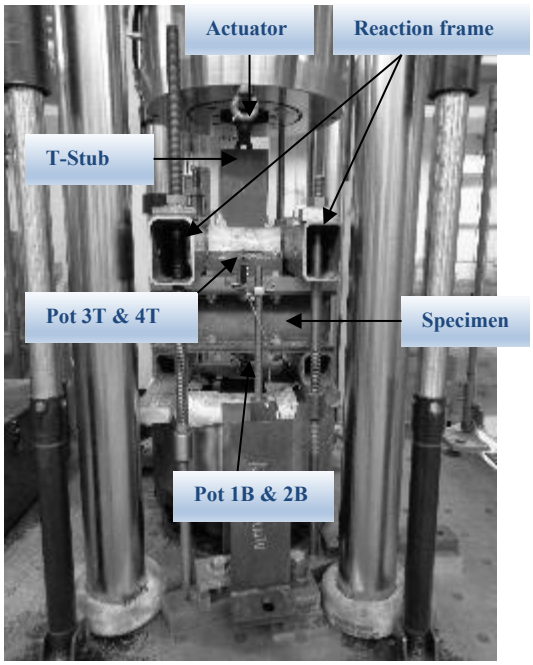

Fig. 2. Test arrangement

2.4. Test setup and loading program

The test arrangement is illustrated in Fig. 2. All specimens were tested under monotonic loading conditions, with the load being applied in displacement control, at a rate of 0.0015 mm/sec up to bolts failure.

The sample was fixed by RHS frames to provide reaction forces and anchored to a strong floor. The reaction frames were 340 mm away from each other providing sufficient distance to allow for free concrete cone formation and to eliminate any influence on load distribution near the bolts, preventing the formation of a possible pyramid shape failure surface.

2.5. Material properties

The bolts properties used in the current study had a diameter of 16 mm, grade 8.8, modulus of elasticity, E_y = 207 MPa and the yield and ultimate strength were, f_{yb}=836 MPa and f_{ub} = 931 MPa respectively.

Four concrete mixes with grade C20, C40, C80 of normal weight and C30 for lightweight concrete were used, where the concrete compressive strengths on the day of testing were 22 N/mm^2, 43.2 N/mm^2, 77 N/mm^2 and 30 N/mm^2 respectively. A nominal maximum aggregate size of 10 mm was specified. All cubes were air cured in order to equate with the curing conditions of the actual pull-out specimens. Pull-out specimens were allowed a minimum of 7 days of curing under room temperature conditions.

3. Finite element modelling

A finite element model was developed using Abaqus 6.14 [8]. The following discusses the properties of this model.

3.1. Material models

3.1.1 Material modelling of steel

An elasto-plastic stress-strain relationships was used in the FE model for the bolts and top plate. Their stress-strain relationships were obtained from experimental data.

3.1.2 Material modelling of concrete

The behaviour of the concrete was stimulated by defining Young's modulus of elasticity and Poison's ratio as an elastic model. The concrete Young's modulus (E_c) is a function of the concrete strength. In this research, equations (1) and (2) [9] were used to calculate E_c for each concrete grade. The Poison's ratio was considered to be 0.2 for all the concrete strengths. The plastic behaviour of the concrete was modelled using a Concrete damage plasticity (CDP) in tension and compression.

$$E_c = 22000\left(\frac{f_{cm}}{10}\right)^{0.3} \quad (1)$$

$$f_{cm} = f_{ck+8} \quad (2)$$

Where

f_{cm}: mean value of concrete cylinder compressive strength

f_{ck}: concrete characteristic compressive cylinder strength

3.2. Finite element model description

The model of EHB comprises six major components but for simplicity, only screw, sleeves, conical nut and anchor nut were implemented as shown in Fig. 3. The model consists of EHB, concrete and top plate. To reduce the time of analysis and geometry modelling, the advantage of symmetry was considered and only a quarter of the sample was modelled. A 20-node quadratic brick element with reduced integration (C3D20-R) is used to mesh the screw and anchor nut. Local seeds with fine mesh were assigned at the bolt shank to detail the stress distribution around the failure region. The sleeves, top plate and concrete are

meshed using 8 node linear brick with reduced integration (C3D8R). The model contains (1) 690 elements for the screw; (2) 780 elements for the sleeves; (3) 80 elements for the sleeves; (4) 1013 elements for concrete; and (5) 172 elements for the top plate.

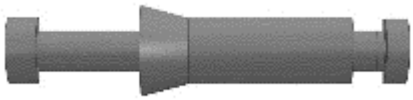

Fig. 3. Finite element model for EHB

The degrees-of-freedom in all side of the concrete are constrained against any translation along all directions as shown in Fig. 4. Also, the degrees-of-freedom in the Z-direction is constrained. To resemble the reaction support (150 x 100 mm), a distance 100 mm from the end is constrained against any translation along all directions.

The contact surfaces in the present model are divided into three groups: contact between the concrete surrounding the embedded screw and sleeves, contact between the below top plate and concrete and contact between clearance hole with sleeves. Both of the normal and the tangential contact exist in the present model. Normal contact needs only defining the surfaces and link them, but in tangential contact the friction modulus should be specified. The coefficient of friction between steel and concrete was considered as 0.25 [10] and between steel and steel was considered as 0.45 [11]. In order to permit full transfer of loads, surface based tie constraint are used between the screw and anchor nut and between screw and sleeves.

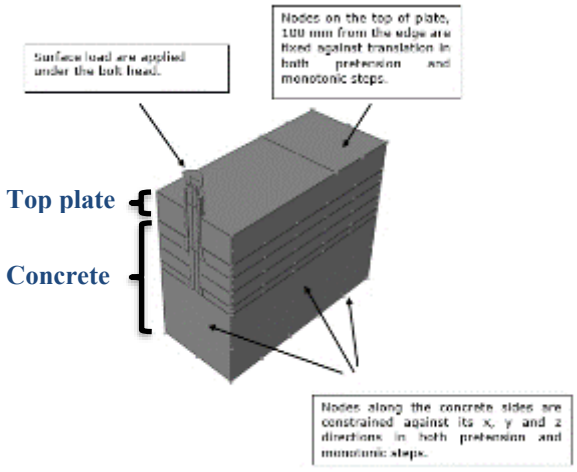

Fig. 4. Boundary conditons

4. Results and discussion

4.1. Failure mode

The concrete-filled region of the EHB failed by bolt shank fracture. A closer examination of the surface of the concrete at the loaded end of the pull-out specimens revealed that the failure also involves concrete cracking between the bolts and at the edges near to the bolts as depicted in Fig. 5. The failure mode did not involve a concrete breakout; it is assumed that the full development of the formation concrete cone occurs before the ultimate capacity of the steel side wall, which acts to confine the concrete cone and prevent concrete breakout from occurring [12]. The concrete cone formation as shown in Fig. 6 also demonstrates the influence of the mechanical anchorage with respect to the distribution of tensile force within the concrete section. The angle of failure slope of 35^0 [13] was assumed off from the horizontal but varied between 30-40 degrees depending of the embedment depths [14] as shown in Fig. 7. Furthermore, the contribution of mechanical anchorage plays a significant role in reducing the amount of deformation in the expanding sleeves

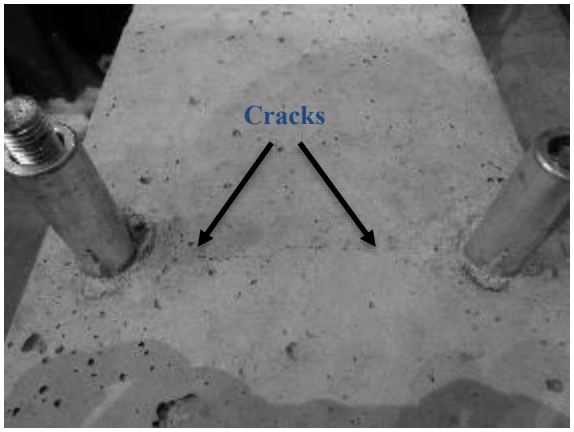

Fig. 5. After testing of EHB in concrete C20 with visible crack running between two bolts

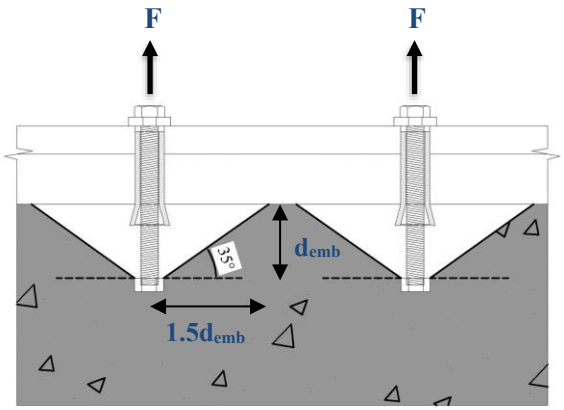

Fig. 6. Concrete cone formation

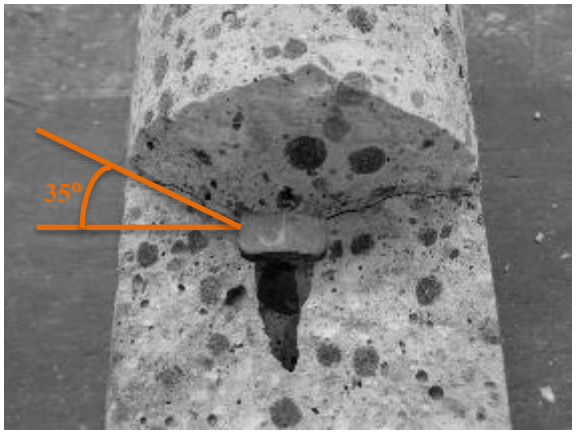

Fig. 7. Concrete cone angle

4.2. Force-displacement relationship

4.2.1 Effect of Bolt Gauge Distance

The effect of bolt gauge on the EHB behaviour was tested using specimens (i) 1-3 with C20, d_{emb} = 66 mm; (ii) 9-11 with C20, d_{emb} = 76 mm; (iii) 12-14 with C20, d_{emb} = 86 mm. As expected, a smaller bolt gauge distance results in lower stiffness while a larger bolt gauge distance results in higher stiffness, as shown in Fig. 8. This might be due to the anchorage contribution since the bolts react individually when the bolts are far apart. However, for low values of gauge distance, the bolts tend to interact and transfer the pressure towards each other which results in lower stiffness due to the lower contribution of the anchorage. Moreover, there is also the edge effect, where if the bolt is close to the edge, it is in a stiffer area, causing it to develop into a strut and tie model.

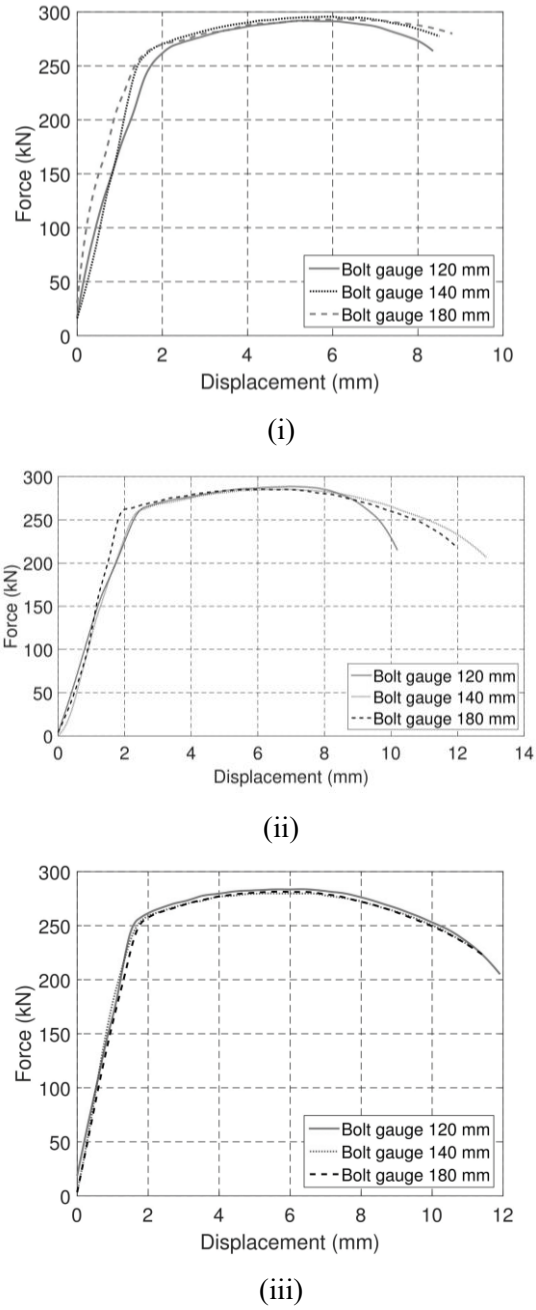

Fig. 8. Effect of bolt gauge distance for 120 mm, 140mm and 180mm for different concrete strengths & embedment lengths

4.2.2 Effect of Concrete Grade (f_{cu})

The effect of the concrete grade on EHB was, tested using specimen 1, 4,6,15 and 18 and is shown in Fig. 9. It can be seen that stiffness of the EHB is significantly influenced by concrete grade. It is found that while the initial stiffness is not significantly affected in the case of increasing the concrete grade from C20 to C80, it can be seen that higher concrete grade enhances the post initial stiffness. The failure mode and failure loads of the EHB are found to be unaffected by changes in concrete grade. All

failure loads correspond to the internal bolt shank.

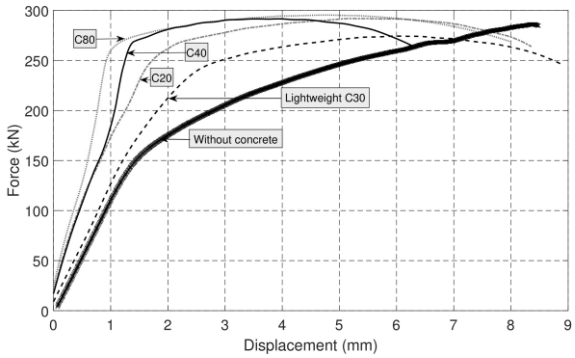

Fig. 9. Effect of concrete grade

4.2.3 Effect of Embedment Depth

The response of the EHB component with varying embedment depth, d_{emb}, was tested using specimen 1, 9 and 12 and the result is shown in Fig. 10. It is indicated that the initial stiffness of the component is significantly affected with the variation in d_{emb}. The ductility of the component is also observed to be affected by the variation of d_{emb}, but the failure mode of the component did not alter as all specimen failed by shank fracture upon reaching ultimate capacity.

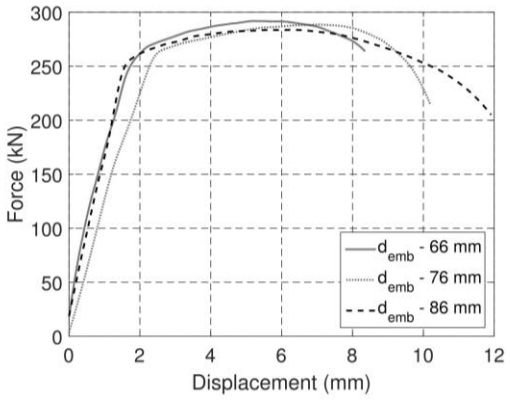

Fig. 10. Effect of embedment depth

4.3. Verification of the model

A comparison of experimental and FEM load-deflection curves is shown in Fig. 11. It can be seen that the FE model has a good agreement with the FE results.

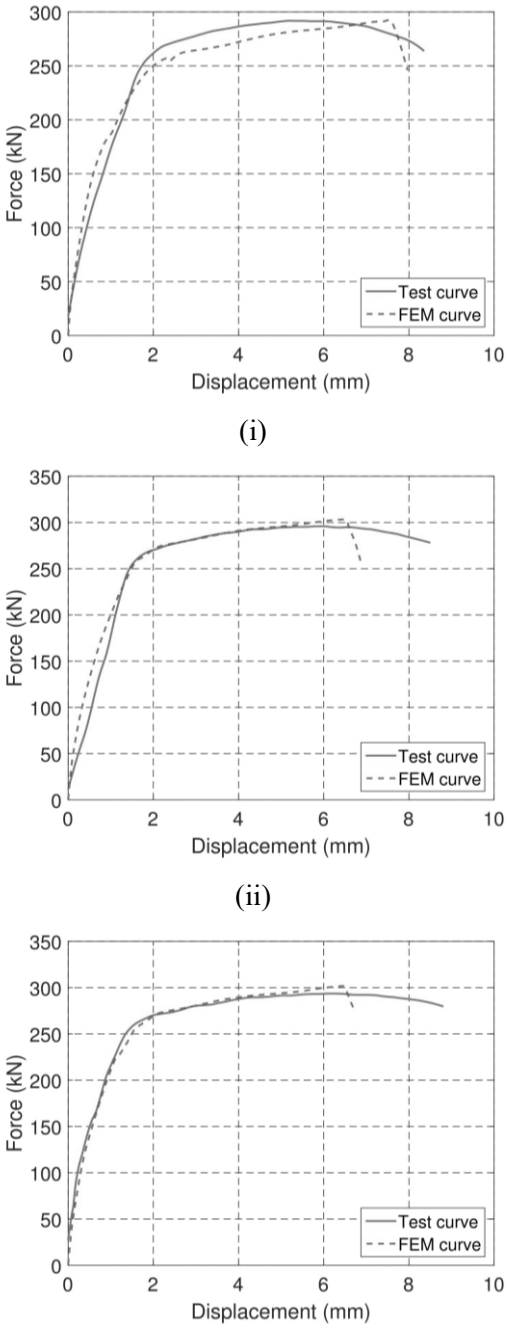

Fig. 11. Validation of FE model for EHB (i) Sample 1; (ii) Sample 2 (iii) Sample 3

Table 2 summarizes a comparison between the ultimate load of the EHB from experimental tests and FE analysis. The maximum loads obtained from the FEM simulated results are found to be consistently lower than the experimental values, although the largest percentage difference is only 2.5%.

Table 2. Ultimate capacity of the EHB experimental and FE results

Sample	Max. load (kN)		% Difference
	Exp.	FE	
1	299.50	292.14	2.5
2	303.65	303.16	0.16
3	301.45	301.24	0.07

5. Conclusions

Tensile pull-out testing of the EHB blind-bolt component has revealed that this component can develop the ultimate capacity of its bolt shank. This is due to the presence of the anchorage mechanism that provides resistance in combination with the sleeve mechanism. This combined action attributes to the ability of the anchor head to transfer the load to the concrete infill.

The concrete compressive strength was found affecting the stiffness of the EHB component. However, the improvement of initial stiffness decreased with the increase of the concrete grade. For concrete compressive strength higher than 40 N/mm^2, the initial stiffness improvement was minor.

The bolt gauge distance (120, 140 & 180 mm) has a significant influence on the stiffness and ductility of the EHB component. The rate of stiffness increases when larger gauge distance is used, whereas the ductility reduced with the use of large bolt gauge distance. However, it is important to consider the influence of concrete strut developing on the side closer to the corner of the section for EHB for large gauge distance. [15].

The other main parameters such as bolt class and pitch distance will be considered in future studies. Comprehensive parametric studies will be implemented using Finite Elements analysis.

A further development of the analytical modelling is necessary to cover all the major parameters that influence the behaviour of the EHB component.

References

[1] Tizani W, and Ridley-Ellis D J. The performance of a new blind-bolt for moment-resisting connections. Proceedings of the 10th international symposium on tubular structures, ISTS 2010: 395-400.

[2] Ellison S, and Tizani W. Behaviour of blind bolted connections to concrete filled hollow sections. The Structural Engineer 2004;82(22): 16-17.

[3] Pitrakkos T, and Tizani W. A component method model for blind-bolts with headed anchors in tension. J. of Steel and Composite Structures 2015;18(5):1305-1330

[4] Tizani W, and Pitrakkos T. Performance of T-Stub to CFT Joints Using Blind Bolts with Headed Anchors. ASCE Journal of Structural Engineering 2015;141(10).

[5] Mollazadeh MH, Wang YC. New insights into mechanism of load introduction into concrete-filled steel tubular column through shear connection. Engineering Structures 2014; 75:139-151.

[6] Morino S, and Tsuda K. Design and Construction of Concrete-filled Steel Tube Column System in Japan. Earthquake Engineering and Engineering Seismology 2004;4(1):51-73.

[7] Wu LY, Chung LL, Tsai SF, Shen TJ, and Huang GL. Seismic behavior of bolted beam-to-column connections for concrete filled steel tube. Engineering Structures 2013;49:876-892.

[8] Abaqus, Inc. ABAQUS Analysis User's Manual 2014. Dassault Systèmes.

[9] CEN. Eurocode 2: Design of Concrete Structures: Part 1-1: General Rules for Buildings, EN 1992-1-1, British Standards Institution.

[10] Elremaily A, and Azizinamini A. Design Provisions for Connections between Steel Beams and Concrete Filled Tube Columns. Journal of Constructional Steel Research 2001;57(9):971-995.

[11] Mahmood M, Tizani W, and Sansour C. Effect of tube thickness on the face bending for blind-bolted connection to concrete filled tubular structures. International Journal of Civil, Architectural, Structural and Construction Engineering 2014;8:904-910.

[12] Oktavianus Y, Hongfei C, Goldsworthy HM, Gad EF. Component model for pull-out behaviour of headed anchored blind bolt within concrete filled circular hollow section. Engineering Structures 2017;148(C):210-224.

[13] Pallarès L. and Hajjar JF. NSEL report series: Headed Steel Stud Anchors in Composite Structures: Part II – Tension and Interaction 2009.

[14] Rao GA, and Sundeep B. Strength of bonded in concrete in direct tension [Online]. Available: https://www.researchgate.net/publication/268010757_Strength_of_bonded_anchors_in_concrete_in_direct_tension 2018.

[15] Agheshlui H, Goldsworthy H, Gad E, Fernando S. Tensile behaviour of anchored blind bolts in concrete filled square hollow sections. Materials and Structures 2016;49(4):1511-1525.